Controlled Shape Deformations via Medial Profiles

Ghassan Hamarneh[1,3]
ghassan@s2.chalmers.se

Tim McInerney[2,3]
tmcinern@scs.ryerson.ca

[1]Department of Signals and Systems
Chalmers University of Technology
Göteborg 412 96, Sweden

[2]School of Computer Science
Ryerson Polytechnic University
Toronto M5B 2K3, Canada

[3]Department of Computer Science
University of Toronto
Toronto M5S 3H5, Canada

Abstract

Robust, automatic segmentation and analysis of medical images requires powerful and flexible models of anatomical structures. We present a multiscale, medial-based approach to shape representation and controlled deformation in an effort to meet these requirements. We use medial-based profiles for shape representation, which follow the geometry of the structure and describe general, intuitive, and independent shape measures (length, orientation, and thickness). Controlled shape deformations (stretch, bend, and bulge) are obtained either as a result of applying deformation operators at certain locations and scales on the medial profiles, or by varying the weights of the main variation modes obtained from a hierarchical (multiscale) and regional (multi-location) principal component analysis of the medial profiles. We demonstrate the ability to produce controlled shape deformations on a medial-based representation of the corpus callosum. Furthermore, we present results of segmenting the corpus callosum in 2D mid-sagittal MRI slices of the brain.

1 Introduction

Controlling the deformations of an object's shape in a way that is based on the natural geometry of the object is highly desirable in image interpretation tasks, especially in the segmentation of natural objects from medical images. This intuitive deformation ability reflects the flexibility of clay to be shaped in a sculptor's hands and naturally lends itself to guidance by high-level controllers. Furthermore, the performance of the controllers can be greatly enhanced by keeping the deformations consistent with prior knowledge about the possible object shape variations.

Most deformable shape models (see [1] for a comprehensive survey) are boundary-based and although provide excellent local shape control, lack the ability to undergo intuitive global deformation. As a result, it is difficult to incorporate intelligent deformation control operating at the right level of abstraction into the typical deformable model framework of energy minimization. Consequently, these models remain sensitive to initial conditions and spurious image features in image interpretation tasks.

Various hierarchical versions of boundary-based deformable models have been developed [2-5] but again fail to provide a natural global description of an object - the multiscale deformation control is constructed upon arbitrary boundary point sets and not upon object-relative geometry. Several global or "volume-based" shape representation or deformation mechanisms do exist [6-10] but are limited either by the type of objects they can model, or the type and intuitiveness of the deformations they can carry out. They are also typically not defined in terms of the object but rather the object is unnaturally defined (or deformed) in terms of the representation or deformation mechanism.

Deformable models based on medial shape representations of objects are emerging as a powerful alternative to boundary-based and volume-based techniques, primarily led by the work of Pizer's group at the University of North Carolina at Chapel Hill [11-13]. Medial representations provide both a local and global description of shape. Deformations defined in terms of a medial axis are natural and intuitive and can be limited to a particular scale and location along the axis.

In this paper, we utilize medial-based *profiles* for shape representation and define deformation operators in terms of these shape profiles. Our goal is the ability to intelligently control the different types and extents of model deformations during the model-to-data fitting process in an effort to focus on the extraction of stable image features before proceeding to object regions with less well-defined features.

To this end, we construct a model of an anatomical structure with a set of profiles that are based on the medial axis of the structure, where each profile describes general and intuitive shape measures (length, orientation, and thickness). Structure deformations (stretch[1], bend, and bulge[2]) are then implemented as deformation operators acting on the shape profiles,

[1] Stretch or compress.
[2] Bulge or squash.

where each operator can have a different shape and scale and can be applied at any point along a profile.

In addition to the general deformation operators, we would also like to use as much knowledge as possible about the object itself and to generate statistically-proven feasible deformations from a training set. We would like to control these statistical deformations locally along the medial shape profiles to support our goal of intelligent deformation scheduling. Since general statistically-derived shape models only produce global shape variation modes [14-15], we have developed spatially-localized feasible deformations at desired scales by utilizing hierarchical (multiscale) and regional principal component analysis to capture shape variation statistics.

In the following sections, we demonstrate the ability to produce controlled shape deformations by applying them to medial-based representations of the corpus callosum (CC), derived from 2D mid-sagittal MRI slices of the brain. We begin by describing the generation and use of medial-based profiles for shape representation and describe a set of general operators that act on the medial shape profiles to produce controlled shape deformations. We then present a technique for performing a multiscale multi-location statistical analysis of the shape profiles and describe statistics-based deformations based on this analysis. In Section 3, we present a simple application of the controlled shape deformations and demonstrate their use in an automatic medical image analysis system. In Section 4, we conclude the paper and provide a brief discussion of several outstanding issues and future work.

2 Shape Representation and Deformation with Medial Profiles

To control shape deformation intuitively requires a shape representation that, among other things, describes global shape variation intuitively. To meet this requirement, we represent the shape with a set of profiles that are based on a sampled medial axis of an object. Each profile captures an intuitive measure of shape: length, orientation, and thickness. Once the profiles are constructed, various deformation functions or *operators* can be applied to a profile, producing intuitive, controlled deformations: stretching, bending, and bulging.

2.1 Medial Profiles for Shape representation

We use a boundary representation of an object to generate the medial-based profiles. Generation of the profiles begins with the extraction of a sampled (semi-automatically) pruned skeleton of the object to obtain a set of medial nodes. Four medial profiles are constructed: a length profile $L(m)$, an orientation profile $O(m)$, a left (with respect to the medial axis) thickness profile $T^l(m)$, and a right thickness profile $T^r(m)$, where $m = 1,2,\ldots,N$, N is the number of medial nodes, and nodes 1 and N are the terminal nodes. The length profile represents the distances between consecutive pairs of medial nodes, and the orientation profile represents the angles of the edges connecting consecutive pairs of medial nodes (measured with respect to the horizontal). The thickness profiles represent the distances between medial nodes and their corresponding boundary points on both sides of the medial axis (Figure 1). Corresponding boundary points are calculated by computing the intersection of a line passing through each medial node in a direction normal to the medial axis, with the boundary representation of the object. Example medial profiles are shown in Figure 2.

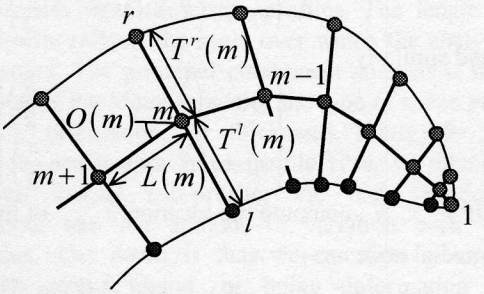

Figure 1. Diagram of shape representation.

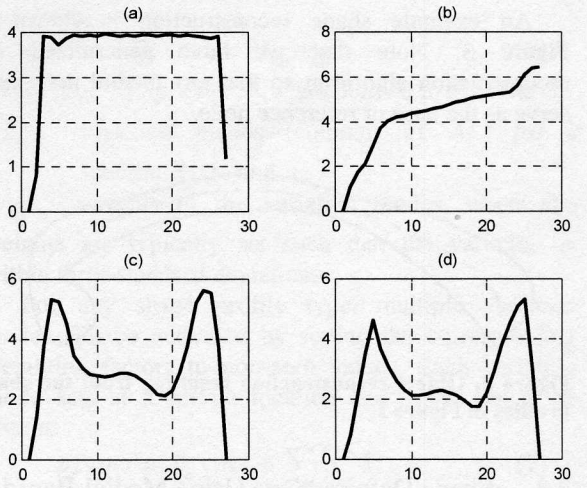

Figure 2. Example medial shape profiles: (a) length profile $L(m)$, (b) orientation profile $O(m)$, (c) left thickness profile $T^l(m)$, and (d) right thickness profile $T^r(m)$.

2.2 Shape Reconstruction from Medial Profiles

To reconstruct the object's shape given its set of medial profiles, we calculate the positions of the medial and boundary nodes by following these steps:

1. Specify affine transformation parameters: orientation angle θ, translation values (t_x, t_y), and scale (s_x, s_y).
2. Using medial node 1 as the base or reference node, place it at location $x_1 = (t_x, t_y)$.
3. Repeat steps 4 and 5 for $m = 1, 2, \ldots, N$.
4. Compute the locations x_m^l and x_m^r of the boundary points l and r at either side of the m^{th} medial node (Figure 1) as

$$x_m^l = x_m + T^l(m) \begin{pmatrix} s_x \cos\left(\theta + O(m) + \frac{\pi}{2}\right) \\ s_y \sin\left(\theta + O(m) + \frac{\pi}{2}\right) \end{pmatrix} \quad (1)$$

and similarly,

$$x_m^r = x_m + T^r(m) \begin{pmatrix} s_x \cos\left(\theta + O(m) - \frac{\pi}{2}\right) \\ s_y \sin\left(\theta + O(m) - \frac{\pi}{2}\right) \end{pmatrix} \quad (2)$$

5. If $m < N$, compute the location x_{m+1} of the next medial node $m+1$ as

$$x_{m+1} = x_m + L(m) \begin{pmatrix} s_x \cos(\theta + O(m)) \\ s_y \sin(\theta + O(m)) \end{pmatrix} \quad (3)$$

An example shape reconstruction is shown in Figure 3. Note that we have generalized the reconstruction algorithm so that any medial node may serve as the base or reference node.

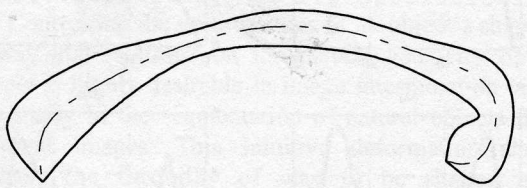

Figure 3. Object reconstruction resulting from the shape profiles in Figure 2.

2.3 Shape Deformations Using Medial-Based Operators

Once the shape profiles have been generated, we can construct deformation operators and apply these operators to the shape profiles. This results in intuitive deformations of the object upon reconstruction. That is, by applying an operator to the length, orientation, or thickness shape profile, we obtain a stretch, bend, or bulge deformation, respectively.

Each deformation operator is implemented by defining a medial-based operator profile, $k(m)$, of a particular type (Figure 4) and specifying an amplitude, location, and scale.

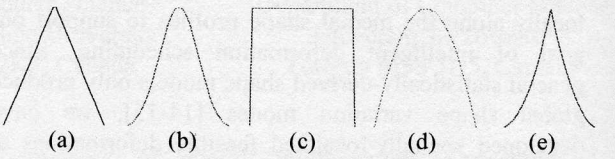

Figure 4. Examples of operator types: (a) Triangular, (b) Gaussian, (c) flat, (d) bell, and (e) cusp [16].

The operator profile is then added to (or blended with) the medial shape profile corresponding to the desired deformation. For example, to introduce a bulge on the right boundary, an operator profile with a specific amplitude, type, location, and scale is generated and added to the right thickness medial profile $T^r(m)$ to obtain $T^r(m) + k(m)$ (Figure 5).

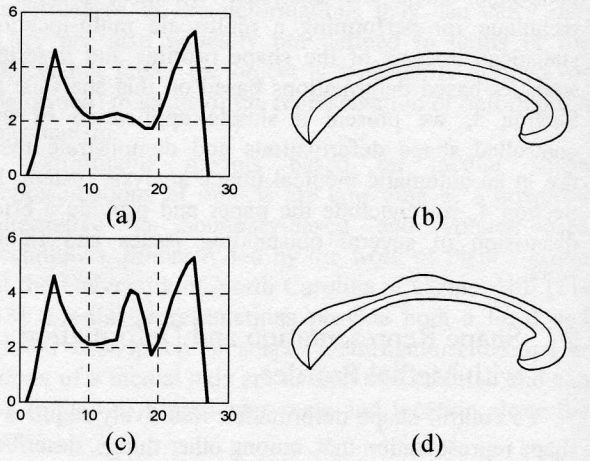

Figure 5. Introducing a bulge on the right boundary by applying a deformation operator on the right thickness profile: (a) $T^r(m)$ before and (c) after applying the operator. (b) The reconstructed shape before and (d) after the operator.

In general the application of a deformation operator $k(m)$ alters the desired shape profile according to

$$p_d(m) = \overline{p}_d(m) + \alpha_{dlst} k_{dlst}(m) \quad (4)$$

where

- p shape profile
- d deformation type (stretch, bend, left/right bulge), i.e. $p_d(m) : \{L(m), O(m), T^l(m), T^r(m)\}$
- $\overline{p}$ average shape profile
- k operator profile (with unity amplitude)

l location
s scale
t operator type (Gaussian, triangular, …, etc.)
α operator amplitude.

Altering one shape profile only affects the shape property associated with that profile and does not affect any other object shape properties. For example, applying an operator to the orientation profile results in a bend deformation only and does not result in a stretch or bulge. This implies the ability to perform successive operator-based object deformations of varying amplitudes, types, locations or scales, which can be expressed as

$$p_d(m) = \overline{p}_d(m) + \sum_l \sum_s \sum_t \alpha_{dlst} k_{dlst}(m). \quad (5)$$

Examples of operator-based deformations are shown in Figure 6a-d.

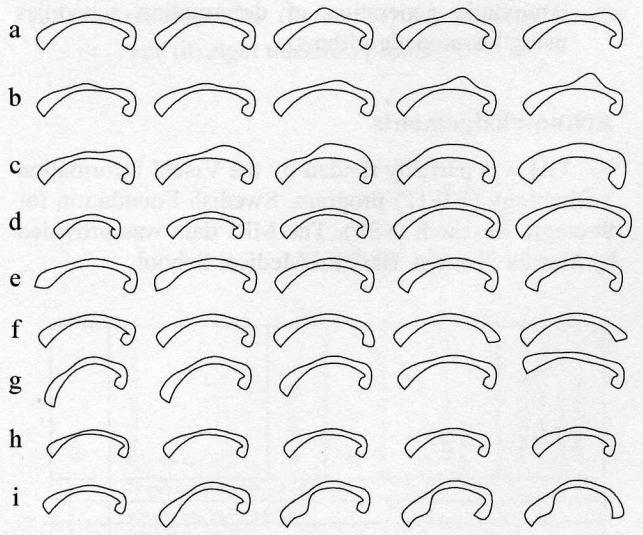

Figure 6. Examples of controlled deformations: (a)-(c) Operator-based bulge deformation at varying locations, amplitudes, and scales. (d) Operator-based stretching with varying amplitudes over entire CC. (e)-(g) Statistics-based bending of the left end, the right end, and the left half of the CC. (h) Statistics-based bulge of the left and right thickness over the entire CC. (i) from left to right: (1) mean shape, (2) statistics-based bending of the left half, followed by (3) locally increasing the left thickness using an operator, followed by (4) applying an operator-based stretch and (5) an operator based bend to the right side of the corpus callosum.

2.4 Statistical Shape Analysis by Hierarchical Regional PCA

In many applications, prior knowledge about object shape variability is available or can be obtained by studying a training set of shape examples. The training set is typically created by labeling corresponding landmark points in each shape example. Principal Component Analysis (PCA) is then applied to the training set, resulting in a point distribution model (PDM) [14]. The PDM describes the main modes of variation of the landmark positions and the amount of variation each mode explains. A drawback of this original approach is that the result of varying the weight of a single variation mode generally causes all the landmark positions to change. In other words, although the original PDM model produces only feasible shape deformations, a desirable trait, it generally produces global deformations over the entire object.

Our goal is to utilize prior knowledge and produce feasible deformations, while also controlling the scale and location of these deformations. Towards this end we perform a multiscale (hierarchical) multi-location (regional) PCA on a training set of medial shape profiles.

To achieve this, we collect spatially corresponding sub-profiles from the shape profiles. The length of a sub-profile reflects the scale over which the analysis is performed. The principal component analysis is now a function of the location, scale, and type of shape profile (length, orientation, or thickness). Thus, for each location, scale, and shape profile type, we obtain an average medial sub-profile, the main modes of variation, and the amount of variation each mode explains. The result is that we can now generate a feasible stretch, bend, or bulge deformation at a specific location and scale.

A shape profile can now be written as the sum of the average profile and the weighted modes of variation as follows

$$p_d(m) = \overline{p}_d(m) + M_{dls} w_{dls} \quad (6)$$

where $p, d, \overline{p}, p_d(m), l, s$ are defined in (4), and

M_{dls} variation modes (columns of M) for a specific d, l, and s,

w_{dls} weights of the variation modes, where the weights are typically set such that the variation is within three standard deviations.

For any shape profile type, multiple variation modes can be activated by setting the corresponding weighting factors to non-zero values. Each variation mode acts at a certain location and scale, hence we obtain

$$p_d(m) = \overline{p}_d(m) + \sum_l \sum_s M_{dls} w_{dls} \quad (7)$$

In summary, varying the weights of one or more of the variation modes alters the length, orientation, or thickness profiles and generates statistically feasible stretch, bend, or bulge deformations at specific locations and scales upon reconstruction.

Examples of statistics-based deformations are shown in Figure 6e-h.

2.5 Combining Operator- and Statistics-Based Deformations

In general, operator- and statistics-based deformations ((5) and (7)) can be combined as

$$p_d = \overline{p}_d + \sum_l \sum_s \left(M_{dls} w_{dls} + \sum_t \alpha_{dlst} k_{dlst} \right) . (8)$$

It is worth noting that several deformations, whether operator- or statistics-based, may spatially overlap (something that we currently do not restrict). Furthermore, adding profiles of different scales, hence different vector lengths, is possible by padding the profiles with zeros.

Figure 6i shows an example of combining operator- and statistics-based deformations.

3 Application and Results

To demonstrate the potential of our statistics- and operator-based controlled deformations, we handcrafted a deformation schedule for fitting the CC shape model to a mid-sagittal MRI slice of the brain. Figure 7 shows the resulting medial shape profiles after applying the fitting schedule (compare with the initial profiles in Figure 2). The initial and final CC shapes are shown in Figure 8. The schedule steps are shown in Table 1 and the resulting deformed CC shapes for each step of the schedule are shown in Figure 9.

Furthermore, we present (Figure 10) recent automatic segmentation results obtained using an intelligent corpus callosum deformable model [17].

4 Conclusion

We have recently constructed a model-based system that automatically and robustly interprets medical images (i.e. segmentation, registration, matching, analysis) by explicitly searching for and fitting to stable image features. A key component of this system is the ability to intelligently schedule and control the type, location, extent, and order of intuitive model deformations during the fitting process [17]. In this paper we have presented 'medial profiles', a medial-based shape representation that provides this ability. Based on these profiles, we are able to construct deformation operators and generate intuitive localized and multiscale deformation types (stretch, bend, bulge). Furthermore, by introducing hierarchical regional PCA we are able to perform a multiscale multi-location statistical analysis of the shape profiles thus generating statistically feasible versions of these deformations.

To demonstrate our approach, we utilized the controlled shape deformations to fit a CC model to a to mid-sagittal brain MRI slices both manually and automatically.

We are aware of remaining and interesting issues, most of which are currently under investigation and research:

- For 3D shape representation, we anticipate a similar yet more involved scheme of medial-based deformation surfaces, operators, and statistical analysis.
- The boundary near the terminals/end caps of the model requires special consideration to prevent loss of continuity. We currently interpolate a cubic spline through the reconstructed left and right boundary points independently, resulting in a loss of continuity at the terminals/end caps of the model. We are therefore exploring alternative boundary representation methods.
- Incorporation of boundary-based displacements to accommodate objects with irregular boundaries.
- Extension of the approach to handle objects with multiple medial axes (i.e. objects with protrusions).
- Automatic generation of deformation schedules using learning algorithms.

Acknowledgements

GH was partially funded by the Visual Information Technology (VISIT) program, Swedish Foundation for Strategic Research (SSF). The MRI data was provided by Martha Shenton, Harvard Medical School.

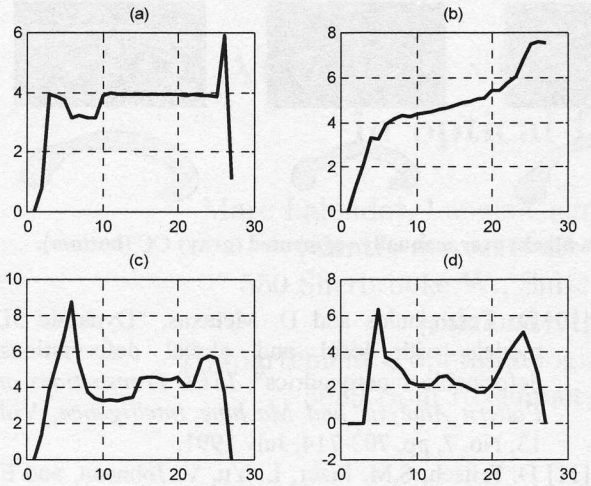

Figure 7. The resulting medial shape profiles after applying the fitting schedule: (a) length profile $L(m)$, (b) orientation profile $O(m)$, (c) left thickness profile $T^l(m)$, and (d) right thickness profile $T^r(m)$.

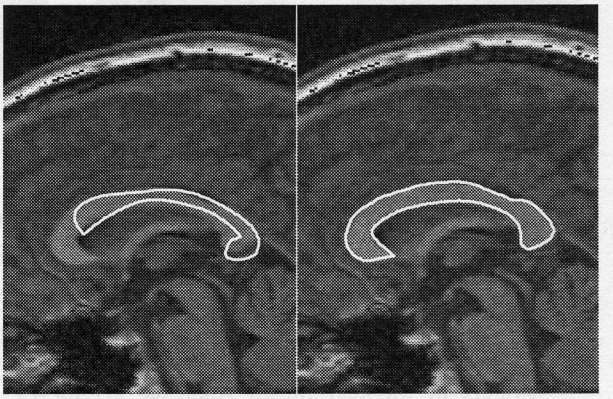

Figure 8. Close up of the initial and final stages of the handcrafted fitting schedule.

Step	Deformation	Location	Scale	Variation mode/ Operator type	Variation mode weight/ Operator amplitude
1	Translation by (▼74,▶24)				
2	Rotation by ↺10°				
3	Scaling by 1.2				
4	Bend	1	8	2	w=0.5
5	Bend	20	8	2	w=-0.8
6	Bend	22	6	2	w=-0.75
7	Bend	24	4	1	w=2.2
8	Bend	1	4	2	w=1
9	Stretch	6	4	1	w=-1.5
10	Stretch	26	1	1	w=2
11	Left-bulge	15	7	1	w=3
12	Left-bulge	18	3	1	w=2
13	Left-bulge	6	12	1	w=3
14	Left-bulge	5	3	1	w=3
15	Right-squash	9	3	1	w=-1
16	Right-bulge	13	2	1	w=0.5
17	Left-bulge	21	3	Gaussian	α=0.3
18	Left-bulge	21	7	Gaussian	α=0.1
19	Right-squash	24	2	Gaussian	α=-0.5
20	Right-bulge	4	2	Bell	α=1.7
21	Right-bulge	6	3	Gaussian	α=0.4
22	Right-squash	1	3	Gaussian	α=-2.2
23	Right-squash	25	1	Gaussian	α=-0.8

Table 1. Deformation schedule used to fit the corpus callosum shape model to the MRI data.

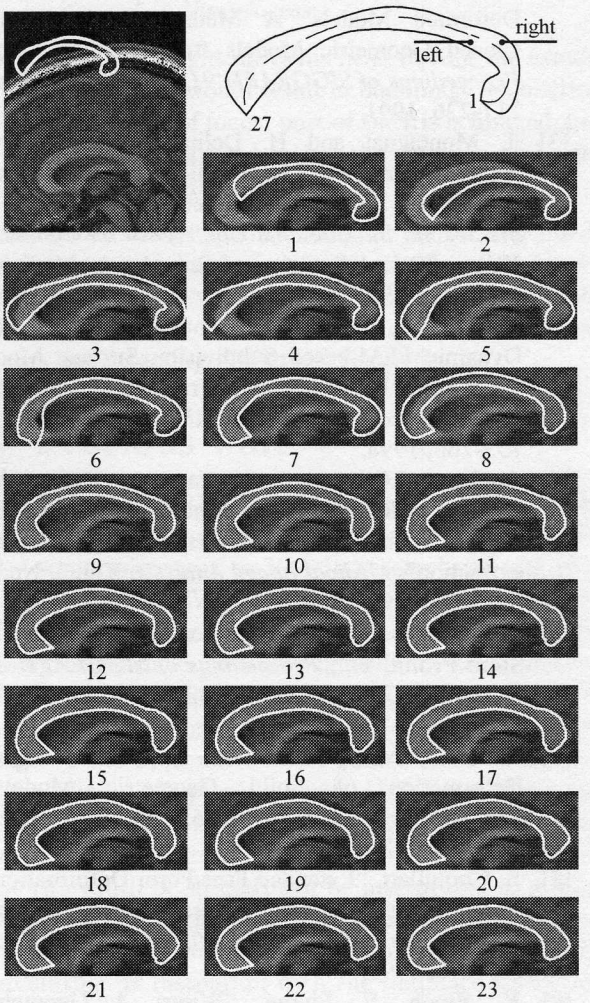

Figure 9. Progress of the handcrafted fitting schedule (fitting steps are listed in Table 1).

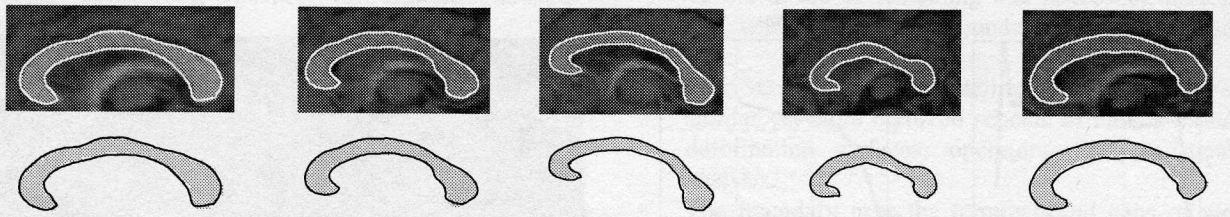

Figure 10. Example segmentation results (top), also shown (in black) over manually segmented (gray) CC (bottom).

References

[1] T. McInerney and D. Terzopoulos, "Deformable Models in Medical Image Analysis: A Survey", *Medical Image Analysis*, Vol. 1, No. 2, pp. 91-108, 1996.

[2] J.V. Miller, D.E. Breen, W.E. Lorensen, R.M. O'Bara, and M.J. Wozny, "Geometrically Deformed Models: A Method for Extracting Closed Geometric Models from Volume Data", *Proceedings of SIGGRAPH'91*, Vol. 25, No. 4, pp. 217-226, 1991.

[3] J. Montagnat and H. Delingette, "Volumetric medical image segmentation using shape constrained deformable models", *Proceedings of the Second International Conference on Computer Vision, Virtual Reality and Robotics in Medicine*, pp. 13-22, 1997.

[4] C. Mandal, B.C. Vemuri, and H. Qin, "A New Dynamic FEM-based Subdivision Surface Model for Shape Recovery and Tracking in Medical Images", *Proceedings MICCAI'98*, Vol. 1496, pp. 753-760, 1998.

[5] Lachaud, J.O. amd A. Montanvert, "Deformable meshes with automated topology changes for coarse-to-fine three-dimensional surface extraction", *Medical Image Analysis*, Vol. 3, No. 1, pp. 1-21, 1999.

[6] A.H. Barr, "Global and Local Deformations of Solid Primitives", *Proceedings of SIGGRAPH'84, Computer Graphics*, Vol. 18, No. 3, pp. 21-30, 1984.

[7] T.W. Sederberg and S.R. Parry, "Free-Form Deformation of Solid Geometric Models", *Proceedings of SIGGRAPH'86*, Vol. 4, No. 20, pp. 151-160, 1986.

[8] S. Coquillart, "Extended Free Form Deformations: A Sculpting Tool for 3D Geometric Modeling", *Proceedings of SIGGRAPH'90*, Vol. 24, No. 2, pp. 187-196, 1990.

[9] K. Singh, E. Fiume, "Wires: A Geometric Deformation Technique", *Proceedings of SIGGRAPH'98*, Vol. 99, No. 1, pp. 405-414, 1998.

[10] D. Terzopoulos and D. Metaxas, "Dynamic 3D models with local and global deformations: deformable superquadrics", *IEEE Transactions on Pattern Analysis and Machine Intelligence*, Vol. 13, No. 7, pp. 703-714, July 1991.

[11] D. Fritsch, S.M. Pizer, L. Yu, V. Johnson, and E. Chaney, "Segmentation of medical image objects using deformable shape loci", *Proceedings of the 15th International Conference on Information Processing in Medical Imaging*, (Lecture Notes in Computer Science), Vol. 1230, pp. 127-140, Springer-Verlag, 1997.

[12] S.M. Pizer, D.S. Fritsch, K.C. Low, and J.D. Furst, "2D & 3D Figural Models of Anatomic Objects from Medical Images", *Mathematical Morphology and Its Applications to Image Processing* (Kluwer Computational Imaging and Vision Series), H.J.A.M. Heijmans, J.B.T.M. Roerdink, Eds. Amsterdam, The Netherlands, pp. 139-150, Kluwer, 1998.

[13] S.M. Pizer and D.S. Fritsch, "Segmentation, Registration, and Measurement of Shape Variation via Image Object Shape", *IEEE Transactions on Medical Imaging*, Vol. 18, No. 10, pp. 851-865, October 1999.

[14] T.F. Cootes, D. Cooper, C.J. Taylor, and J. Graham, "Active Shape Models – Their Training and Application", *Computer Vision and Image Understanding*, Vol. 61, No. 1, pp. 38-59, 1995.

[15] G. Szekely, A. Kelemen, Ch. Brechbuehler, and G. Gerig, "Segmentation of 3D objects from MRI volume data using constrained elastic deformations of flexible Fourier surface models", *Medical Image Analysis*, Vol. 1, No. 1, pp. 19-34, 1996.

[16] J.R. Bill and S.K. Lodha, "Sculpting Polygonal Models using Virtual Tools", *Proceedings of Graphics Interface*, pp. 272-279, 1995.

[17] G. Hamarneh, T. McInerney, D. Terzopoulos, "Intelligent Deformable Organisms: An Artificial Life Approach to Medical Image Analysis", Technical report CSRG-432, Department of Computer Science, University of Toronto, 2001, ftp://ftp.cs.toronto.edu/cs/ftp/csrg-technical-reports/. Also submitted to *MICCAI'2001*.